

Elsevier required licence: © <2020>. This manuscript version is made available under the CC-BY-NC-ND 4.0 license <http://creativecommons.org/licenses/by-nc-nd/4.0/>

The definitive publisher version is available online at

[\[https://www.sciencedirect.com/science/article/pii/S0016236119317910?via%3Dihub\]](https://www.sciencedirect.com/science/article/pii/S0016236119317910?via%3Dihub)

The Effect of Diesel Fuel Sulphur and Vanadium on Engine Performance and Emissions

**Thuy Chu-Van^{1a,2}, Nicholas Surawski³, Zoran Ristovski^{1b,*}, Chung-Shin Yuan⁴, Svetlana Stevanovic⁵,
S. M. Ashrafur Rahman^{1a}, Farhad M. Hossain^{1a}, Yi Guo^{1b}, Thomas Rainey^{1a}, Richard J. Brown^{1a}**

^{1a}Biofuel Engine Research Facility (BERF) –

^{1b}International Laboratory for Air Quality and Health (ILAQH) –

Queensland University of Technology, 2 George St, Brisbane City, Queensland 4000, Australia

²Vietnam Maritime University, 484 Lach Tray St, Hai Phong City 180000, Vietnam

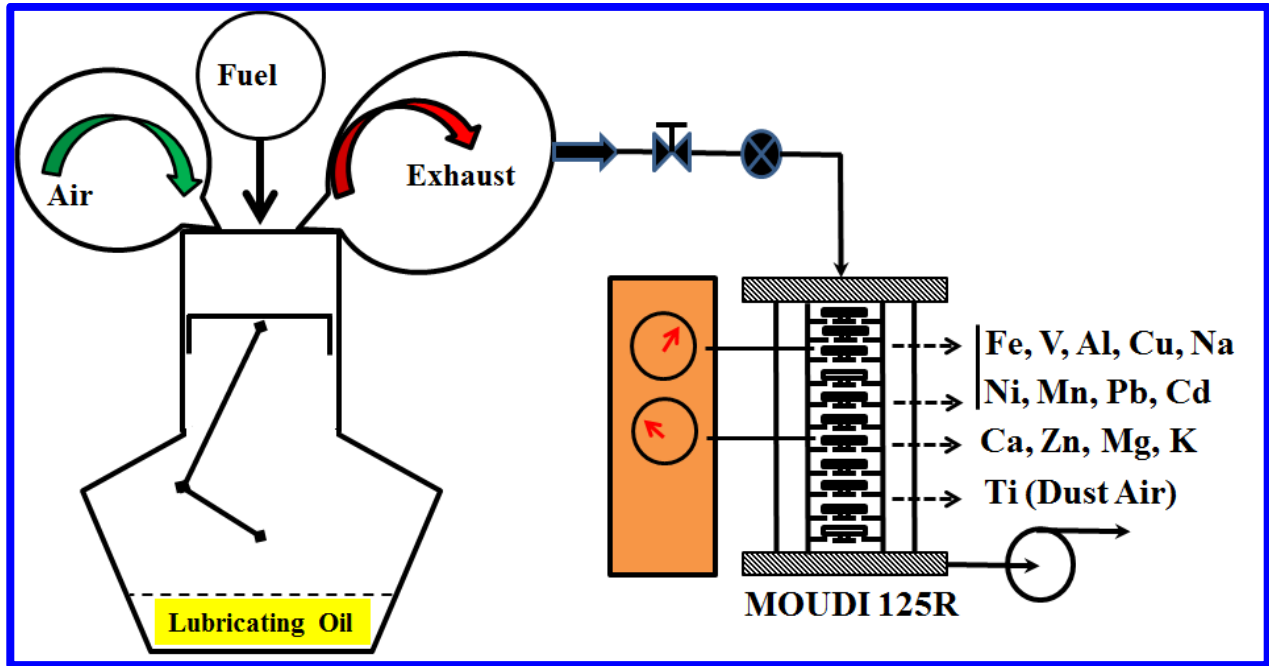
³University of Technology Sydney, 81 Broadway, Ultimo NSW 2007, Australia

⁴National Sun Yat-sen University, 70 Lian-Hi Road, Kaohsiung 804, Taiwan

⁵School of Engineering, Deakin University, 75 Pigdons Road, Victoria 3216, Australia

HIGHLIGHTS

- Source identification of metallic elements in the engine exhaust particles performed;
- Metallic element distributions in exhaust measured at different particle size fractions;
- Lubricant related metals contributed to metallic solid ultrafine particles ($D_p < 100$ nm);
- Fuel and engine wear related metals dominant in the accumulation particle mode;
- Large impacts of engine load on NO_x and fuel S content on PM were found;



20

21

22 **ABSTRACT**

23 Metallic composition of diesel particulate matter, even though a relatively small proportion of total mass, can
 24 reveal important information regarding engine conditions, fuel/lubricating oil characteristics and for health
 25 impacts. In this study, a detailed investigation into the metallic elemental composition at different particle
 26 diameter sizes has been undertaken. A bivariate statistical analysis was performed in order to investigate the
 27 correlation between the metallic element, measured engine performance and engine emission variables. Major
 28 sources of metallic elements in the emitted particles are considered in this study, including the fuel and
 29 lubricating oil compositions, engine wear emissions and metal-containing dust in the ambient air. Metallic solid
 30 ultrafine-particles ($D_p < 100$ nm) are strongly associated with metallic compounds derived from lubricating oil
 31 (Ca, Zn, Mg and K), while the fuel related metallic compounds and engine wear emissions are represented in
 32 the accumulation mode particle fraction (> 100 nm). Calculated correlation matrices show a clear effect of
 33 engine load conditions and fuel S contents on particle number and mass emissions.

34

35 **Key words:** Sulphur, Vanadium, Particle Size Distributions, Metallic Element Distributions, Micro-Orifice
 36 Uniform Deposition Impactors (MOUDI).

37 **1. Introduction**

38

39 Marine fuels such as marine diesel oil (MDO) and heavy fuel oil (HFO) are the main fuels used in the shipping
40 industry. This industry accounts for over 80% of global trade by some 90,000 marine vessels [1]. Using low
41 quality marine fuels, owing to their economic benefits [2] significantly contributes to worldwide air pollution
42 and air quality degradation in the vicinity of coastal and port areas [1, 3]. Sulphur (S) and many trace metals
43 and other chemical elements such as silicon (Si), nickel (Ni), iron (Fe), lead (Pb), aluminum (Al), calcium (Ca)
44 and vanadium (V) are observed in marine fuels, so marine fuel combustion consequently results in different
45 compounds like sulfates, organic carbon (OC), elemental or black carbon (EC/BC), ash and heavy metals in
46 emitted particles [4-6], most of which pose a high toxicity risk [7]. It is well documented that inhaling diesel
47 particulate matter is a very significant health risk [8]. Based on a detailed review, the International Agency for
48 Research on Cancer (IARC), which is part of the World Health Organization (WHO), classified diesel engine
49 exhaust as a carcinogenic substance to human health (Group 1, same as asbestos) [9]. In particular, shipping-
50 related fine particle (PM_{2.5}) emissions alone can account for nearly 64,000 cardiopulmonary and lung cancer
51 deaths each year [10]. In Europe, 5–10% of total PM emissions derived from ship emissions corresponded to
52 around 40,000 premature deaths per year [11]. Therefore, quantitative and qualitative research on ship emissions
53 is needed for a deeper understanding for law-makers and regulators [12] and is a matter of critical concern [13].

54

55 In the literature, there are three major methods to investigate emissions from ships, namely test-bed, ship plume-
56 based and on-board measurements, in which on-board measurements are essential to fully investigate realistic
57 emission factors [14, 15]. However, a very limited number of on-board measurement studies have been
58 undertaken [13, 16], especially regarding ultrafine particle number, particle chemical composition and the
59 concentration of trace metallic elements in ship exhaust [4, 17]. More fuel parameter-related studies are needed
60 in order to understand emission composition more deeply and to effectively reduce negative health impacts in
61 coastal areas [4]. On-board ship emission measurements are an extremely complex task that needs the
62 participation and availability of a wide range of institutions, as well as modern instruments. Therefore, spiking
63 diesel fuel with S and V is used as an approach to better understand the effect of S and V on engine performance
64 and emissions of auxiliary engines when using fuels containing these components such as diesel or HFO under
65 controlled laboratory conditions [18].

66

67 Emissions from ships are regulated by the International Maritime Organization (IMO) through Annex VI of the
68 International Convention for the Prevention of Pollution from Ships – the Marine Pollution Convention
69 (MARPOL). Regulations came into effect on May 19th 2005 introducing limits on the oxides of nitrogen (NO_x)
70 and the oxides of sulphur (SO_x) emissions in order to reduce harmful pollutants from ships globally. Responding
71 to the desire of some coastal nations for further reduction of SO_x emissions from ships in their regions, Sulphur
72 Emission Control Areas (SECAs) have been instituted by applying provisions contained in the Regulation 14 of
73 MARPOL Annex VI. These regulations limit the marine fuel sulphur content to 0.1% by mass in SECAs by
74 2015, and to 0.5% globally by 2020. As an alternative to using low- sulphur fuel oil, approved systems for the

75 abatement of emissions, such as SO_x (wet and dry) scrubbers are likely to be dominantly used [15]. Scrubber
76 systems play a role as filters of the engine exhaust gasses to remove SO_x by using washing-water that will be
77 discharged directly into ocean (open loop), treated with chemicals and reused for a time before discharging
78 (closed loop), or treated through a hybrid mode of the above [19]. Regulation 13 of MARPOL Annex VI controls
79 NO_x emissions from both used and new marine diesel engines that are over 130 kW output power. Different
80 levers or tiers depend upon the ship construction date and engine speed. It should be noted that Tier III
81 requirements apply only to new vessels operating in Nitrogen Oxide Emission Control Areas (NECAs)
82 established to limit NO_x emissions. Exhaust gas recirculation (EGR) arrangements and selective catalytic
83 reduction (SCR) systems seem to be a feasible abatement technology to achieve NO_x reduction. However, a
84 recent study reported that there were around 500-1000 vessels equipped with SCR [20]. This indicates that the
85 large numbers of existing vessels without exhaust cleaning systems are in operation. Therefore, a diesel engine
86 without after treatment system was used in the present study.

87

88 The chemical composition and physical characteristics of PM depend on fuel types used, the engine type and
89 engine operating conditions [21]. The most abundant components of PM from marine fuel combustion are
90 hydrated sulfates, OC, EC/BC and trace metals with over 80–97% of total PM_{2.5} mass, in which total trace
91 metals accounted for only 1.25–3.87% [17]. Using the V/Ni ratio as a tracer for a ship's emitted particles (those
92 associated with fuel metal content) is an effective way to detect and assess the contribution of ship emissions to
93 ambient air [7, 22]. While primary PM emission elements of Ca, Zn, P and Mg are largely determined by the
94 composition of lubricating oils [23], OC and EC/BC are affected by engine load conditions [21, 24]. In the
95 literature, the presence of trace metals deposited in emitted PM is poorly investigated [16, 17] and there are few
96 studies concerning metallic elements on particles of different sizes.

97

98 In this research, test-bed measurements were performed on a heavy duty, six-cylinder, turbocharged and after-
99 cooled diesel engine with a common rail injection system and without after treatment system in order to provide
100 a detailed insight into the elemental composition at different particle diameter sizes. The engine was tested with
101 spiked diesel fuels with different S and V contents over several engine modes, representing the typical range of
102 in-use operating load conditions. A statistical analysis tool (R studio) was used to calculate correlation matrices
103 investigating relationships between the measured engine performance and emissions variables.

104 2. Methodology

105 2.1. Spiked fuel preparation

106 Fuel S contents selected were 0.1% and 0.5% (by weight) that relate to S regulations issued by IMO applying
107 in both SECAs and NECAs by 2015, and globally by 2020 respectively. Diesel and HFO contain different S-
108 species associated with the differences in the volatility of the two fuels. Some studies stated that S-containing
109 compounds such as dibenzothiophenes are dominant in HFO [25, 26], and in diesel fuel [27]. In contrast,
110 dibenzothiophenes in alkylated structure were found to be dominant in diesel fuel compared to their parent
111 structure [28]. Therefore, dibenzothiophenes have been selected in this study to spike the fuels with S. Typical
112 trace metals which are commonly found in HFO are V and Fe. V is contained in diesel fuels in a soluble form,
113 which is present as vanadium-porphyrin complexes [29]. The typical concentrations of V in HFO strongly
114 depend upon the source of crude oil. Fe-based fuel-borne catalysts have been widely used in Europe as fuel
115 additives to reduce engine emissions [30]. Chemicals containing these metallic elements (V and Fe) were used
116 to spike the fuels as follows: bis(cyclopentadienyl)vanadium (II) and ferrocene. Further details of fuel
117 preparation can be seen in a previous study [18]. The quantity of these chemicals along with diesel fuel used for
118 spiking fuels can be seen in Table S1 (Supporting Information). Details of these chemicals can be seen in Table
119 S2. The properties of spiked fuels can be seen in Table 1.

120

121 **Table 1** Properties of spiked fuels.

Parameters	Units	Methods	Diesel	S0.1V5	S0.1V15	S0.5V5	S0.5V15
Density	g/L	ASTM D4052	837.6 ^a 844.4 ^b	846 ^b	847 ^b	849 ^b	850 ^b
Viscosity	mm ² /s	ASTM D445	2.66 ^a 2.66 ^b	3.12 ^c	3.13 ^c	3.32 ^c	3.35 ^c
Lubricity	mm	IP 350	0.41 ^a	-	-	-	-
Carbon (C)	% mass	-	87.10 ^b	88.78 ^b	88.72 ^b	88.65 ^b	86.25 ^b
Nitrogen (N)	% mass	-	0.054 ^b	0.043 ^b	0.0462 ^b	0.0456 ^b	0.039 ^b
Sulphur (S)	% mass	-	6.1 x 10 ^{-4a} 7.8 x 10 ^{-4b}	0.097 ^b 0.095 ^c	0.095 ^b 0.093 ^c	0.475 ^b 0.497 ^c	0.513 ^b 0.512 ^c
Vanadium (V)	mg/kg	-	<1 ^c	4 ^c	13 ^c	5 ^c	14 ^c
Iron (Fe)	mg/kg	-	<1 ^c	8 ^c	8 ^c	8 ^c	8 ^c
HHV*	MJ/kg	ASTM D240	45.64 ^b	44.16 ^b	44.31 ^b	43.34 ^b	43.68 ^b

122 (a from CALTEX, ^b tested at QUT; ^c from Hasting Deering; * Higher heating value)

123

124 2.2. Engine specifications and experiment set-up

125 This experimental investigation used a heavy duty, six-cylinder, turbocharged, after-cooled diesel engine with a
126 common rail injection system located in the Biofuel Engine Research Facility (BERF) at the Queensland
127 University of Technology. The exact specifications of this engine are presented in Table 2. Further details of the
128 engine specifications can be seen in previous studies [18, 31]. The research engine was tested at a constant speed
129 (1500 rpm) and two engine load conditions (25% and 50% load) which are typical operating conditions of an
130 auxiliary marine engine. Higher engine loads up to 80-90% were not carried out due to the limitations of time
131 and costs of chemicals for spiking fuels. Paper filter was used at the intake air of the engine. Fig. 1 shows a
132 schematic diagram of the experimental setup. The first sampling point was used for raw exhaust measurements

133 by a Testo 350 XL for gaseous concentration including sulphur dioxide (SO₂), nitrogen oxides (NO_x), carbon
 134 monoxide (CO), carbon dioxide (CO₂), oxygen (O₂), and unburned hydrocarbons (HCs). The raw hot-exhaust
 135 was also directed to the DMS500 MKII Fast Particulate Spectrometer (CAMBUSTION, Cambridge, UK) after
 136 a two-stage dilution system (in-built into the instrument) and the CAI NO_x and CO₂ analysers measured from
 137 the second sampling point. Particle number size distributions in the size range of 5 nm–1.0 µm were analysed
 138 with a sampling frequency of 1 Hz using a DMS500 MKII through a heated sample line, and two dilution stages.
 139 The third sampling point was firstly diluted through the dilution tunnel and then used for measurements with a
 140 Micro-Orifice Uniform Deposit Impactor (MOUDI 125R Impactor, MSP Corporation, USA), a DustTrak™ and
 141 a Sable CA-10 carbon dioxide analyser. The MOUDI 125R is a 13-stage cascade impactor that works on the
 142 principle of inertial impaction combined with PTFE Teflon filters for off-line metal concentration measurements
 143 for the emitted particles. A DustTrak™ II Aerosol Monitor 8530 (TSI), which is a light-scattering laser
 144 photometer giving real-time aerosol mass readings, was used to measure mass concentrations of PM₁₀, PM_{2.5}
 145 and PM_{1.0}. Raw and dilute CO₂ measurements were used to determine the sample dilution ratios (DR) for the
 146 DustTrak™ measurements. Further details on the dilution condition are provided in Table S3. A flow rate of 10
 147 L min⁻¹ was fixed for MOUDI 125R sampling, created by a vacuum pump. Details of the sampling line length
 148 and flow rate for other instruments can be seen in Table S4.

149

150 **Table 2** Test engine specifications

Item	Specification
Model	Cummins ISBe220 31
Cylinders	6 in-line
Capacity (Litres)	5.9
Bore x Stroke (mm)	102 x 120
Maximum Torque	820 Nm @ 1500 rpm
Maximum Power	162 kW @ 2500 rpm
Compression Ratio	17.3:1
Aspiration	Turbocharged (waste gated) & after cooled
Injection Type	High pressure common rail
Dynamometer Type	Electronically controlled water brake dynamometer
Emission Standard	Euro IIIA

151

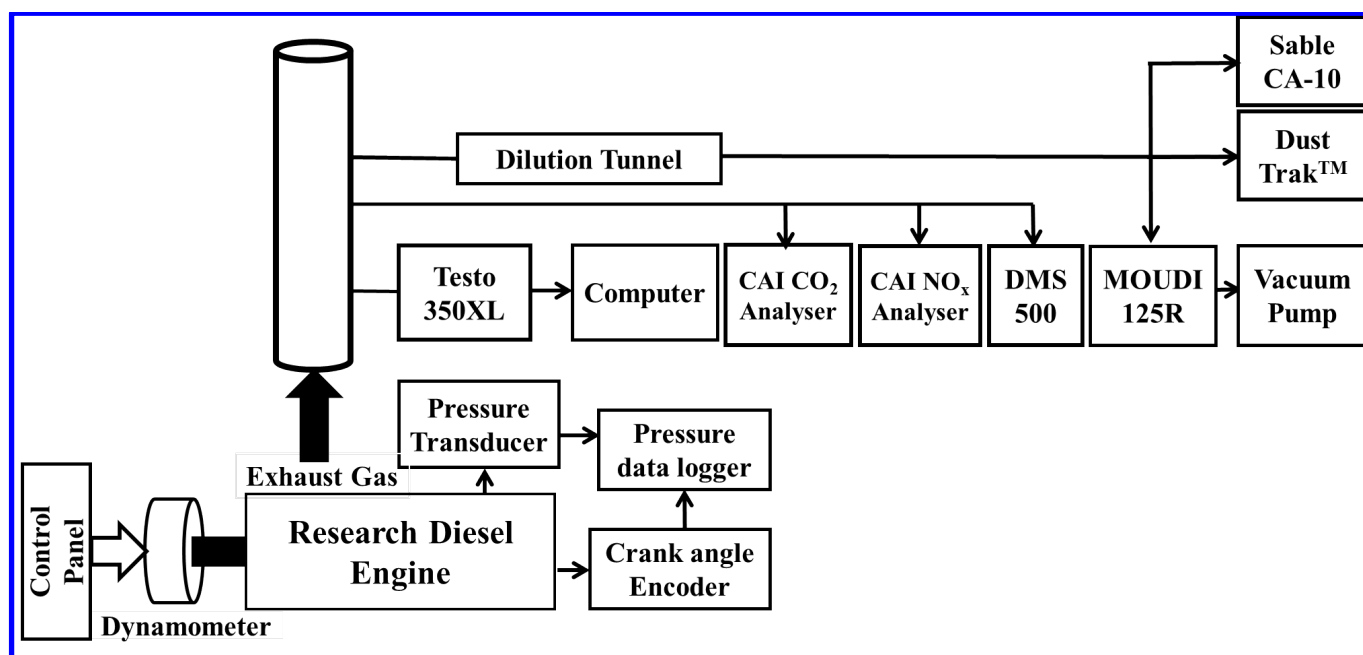


Fig. 1. Schematic diagram of experiment setup

2.3. MOUDI sampling setup and chemical analytical methods

Measurements of the particle mass distribution were done through a 13-stage cascade impactor that works on the principle of inertial impaction [32]. The schematic for particle collection with the MOUDI can be seen in the Supporting Information (Fig. S1). MOUDI impactor classifies particles based on their aerodynamic diameter that is affected by the effective density of particles. The MOUDI was configurational for particulate matter collection in four size fractions (< 10 nm, 10–100 nm, 100–1000 nm, and > 1000 nm). The last stage < 10nm was collected on the backup filter. Due to the characteristics of this instrument the smallest (10 nm) cut-off cannot be known with great precision. The modification of MOUDI can be found in previous studies [33, 34]. The sample was collected for 25 min and deposited on 47 mm diameter 0.45 μm pore Teflon (PTFE) filters (Pall Life Sciences, Ann Arbor, MI). One-eighth of the Teflon filter was initially digested by microwave digestion in a 30 mL mixed acid solution (HNO_3 : HClO_3 = 3:7) by heating it up to 150–200 $^\circ\text{C}$ for 2 hours to extract metals from the collected particles. After the digestion, 50 mL de-ionized (D.I) water was added to the residual solution for metallic content analysis. Seventeen metallic elements consisting of As, Ca, Cd, Cr, Cu, Fe, Mg, Na, Mn, Sb, Ni, Pb, Ti, V, Al, K, and Zn were analysed with an Inductively Coupled Plasma-Atomic Emission Spectrometer (ICP-AES; Perkin Elmer, Model Optima, 2000DV). In order to prevent background contamination in the engine lab, the operational blanks (unexposed filters) were used simultaneously with the exhaust samples. The blank interference was ignored in the present study because of its insignificance found. This chemical analysis was carried out in the Air Pollution Laboratory at National Sun Yat-sen University. The quality assurance and quality control of chemical analysis that were conducted in this study are described in more details in the Supporting Information (Table S5). Further details of this method can also be seen in a previous study [35].

177

178 **2.4. Datasets and their analysis**

179 **2.4.1. Correlation matrices**

180 Correlation matrices were calculated in R [36] to explore the relationship between variables in this study.
181 Correlation co-efficients (r) lie on the interval [-1 1] and are calculated in a pairwise manner for every
182 combination of variables. An r value of 1 indicates perfect correlation, $r=-1$ indicates perfect anti-correlation for
183 a variable pair, whereas an r value of 0 indicates no relationship. Calculations were performed using the corrplot
184 package [37].

185

186 **2.4.2. Datasets analysed**

187 Correlation matrices were calculated in R for two datasets. The first dataset involved the particle-phase metallic
188 concentrations resulting from ICP-AES, while the second dataset analysed the complete dataset consisting of
189 gas and particle phase pollutants as well as engine performance variables. Information regarding replication was
190 retained in analyses of both datasets.

191

192 **3. Results and discussion**

193 **3.1. Identifying sources of metallic elements in the engine exhaust particles**

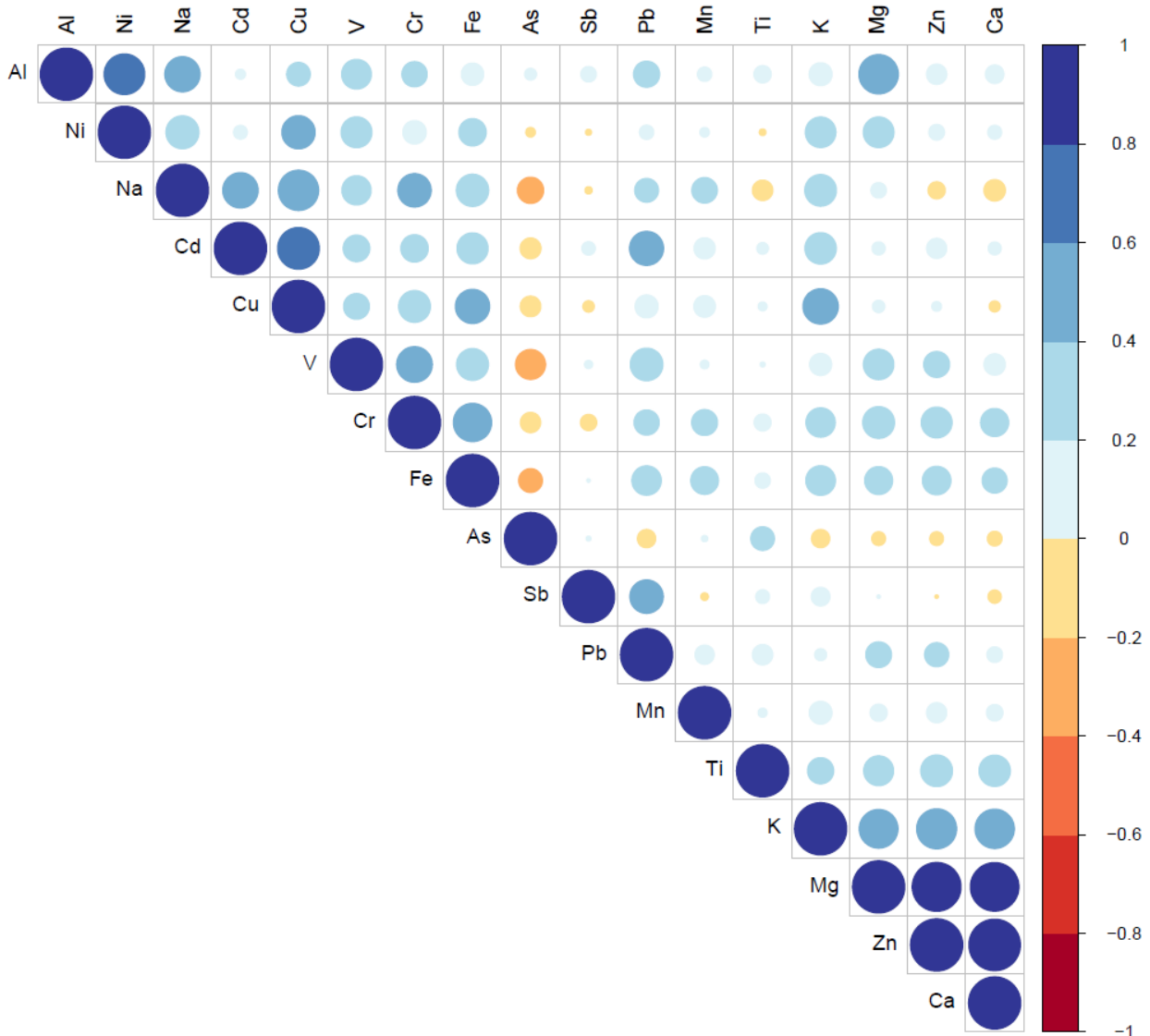
194 Fig. S2 shows obvious potential sources of metals in the particles emitted from the diesel engine exhaust. They
195 come mostly from the composition of fuel burned, lubricating oil used, ambient air and engine wear. Source-
196 specific information should be obtained to determine and confirm directly the major sources of metallic elements
197 in the emitted diesel engine exhaust particles. In particular, seventeen metallic elements consisting of As, Ca,
198 Cd, Cr, Cu, Fe, Mg, Na, Mn, Sb, Ni, Pb, Ti, V, Al, K and Zn from diesel engine exhaust emissions were collected
199 on Teflon filters and were analysed by using ICP-AES. The results of this analysis consisting of different spiked
200 fuels and engine load conditions are presented in Fig. S3. Concentrations of metallic elements from the engine
201 when running reference diesel can be seen in Fig. S4. Elemental analysis for tested fuels, new and used
202 lubricating oil were carried out and the results are presented at Tables S6, S7 and S8 in the Supporting
203 Information. Elemental composition of particles in the ambient air was derived from previous studies [38, 39]
204 and used as a reference in the present study because their work used samples taken in the same city (Brisbane)
205 as this study. The typical metal concentrations in Brisbane ambient air can be seen in Table S9, in which the
206 dominant metallic elements in the ambient air (presented in the red text) are Na, Fe, Ca, K, Zn, Ti and Al. It
207 should be noted that PM concentration and composition in the engine laboratory (in the present study) may
208 differ from that of these studies, which sampled PM at inside schools, outside at suburban areas and roadsides.
209 Therefore, the reference may partly reflect the real world situation.

210

211 **3.2. Correlation of metallic variables in the engine exhaust emissions**

212 Fig. 2 shows the correlation of metallic elements in the engine exhaust emission. In particular, the scale bar is
213 the correlation coefficient (from -1 to 1), the blue symbol indicates that these variables are correlated while the

214 red one represents the anti-correlated variables. In addition, size of symbol illustrates the strength level of
 215 correlation/anti-correlation, for instance, larger circle means stronger their relation is. There are ninety-two
 216 samples in total including all of the engine load conditions (25 and 50%) and tested fuels, which were used to
 217 plot Fig. 2. Based on the interpretation of Fig. 2, it can be seen clearly that there are three separate groups of
 218 variables. Correlated variables included Ca, Zn, Mg and K are strongly associated with lubricating oil, while
 219 elements related to the fuel composition (V, Fe) and engine wear (Fe, Al, Cu, Cr, Pb and Cd) are found in the
 220 same group. Pb and Cd have been reported from engine wear, most likely from piston rod bearings [40, 41].
 221 The last group with elements such as As and Ti that is most likely to be from air dust source or/and engine
 222 cylinder walls. The reason for the present of As in the air is not clear but it is consistent with a previous study
 223 [42] who found As in combustion particles near airport in both large and small sizes. In addition, as be seen in
 224 Fig. 2 that a correlation between As and Ti which is most likely to prove the evidence of As in the air. However,
 225 further work is needed to confirm scientifically this statement because this correlation observed in the present
 226 study is weak (the correlation coefficient of around 0.2-0.25).
 227



228 **Fig. 2.** Correlation matrix of particle phase metallic concentration variables in the engine exhaust emission
 229

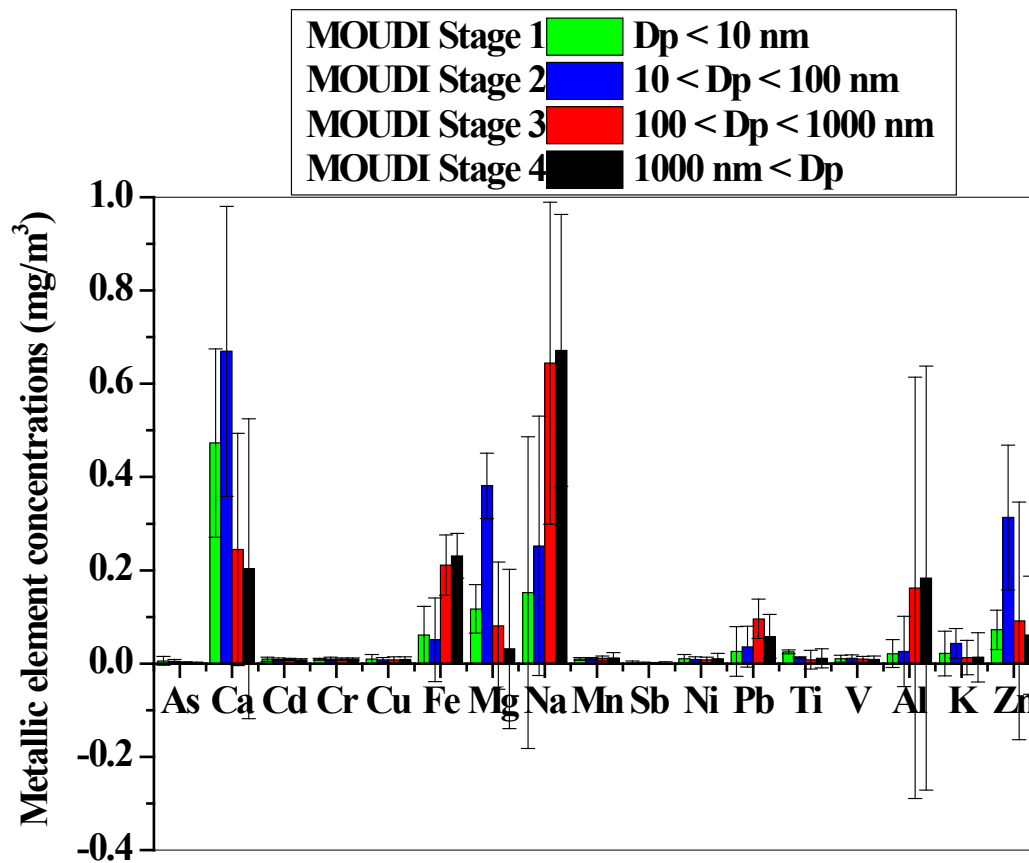
230

231 Fig. 3 shows the metallic element concentrations distributed at four different MOUDI stages including different
232 particle aerodynamic diameters ($D_p < 10$ nm – stage 1; 10 nm $< D_p < 100$ nm – stage 2; 100 nm $< D_p < 1000$
233 nm – stage 3; $D_p > 1000$ nm – stage 4). The results at each MOUDI stage were averaged for the all of engine
234 load conditions and tested fuels in the total of ninety-two samples. MOUDI stages 1, 2, 3 and 4 presented in
235 green, blue, red and black columns, respectively. Based on Fig. 3, the concentration of particular metallic
236 element varies greatly with different MOUDI stages. In particular, it is clearly evident that metallic elements
237 derived from lubricating oil in the emitted particles are strongly associated with the MOUDI stages 1 and 2.
238 They are of Ca, Mg, Zn and K which can normally be found as components in engine lubricating oil (Table S7).
239 It can be concluded that metallic solid ultrafine-particles ($D_p < 100$ nm) of diesel exhaust mainly originate from
240 metallic contents in the lubricating oil. The results in the present study are also in agreement with previous
241 studies for both gasoline engines [43, 44] and diesel engines [45, 46]. A recent study [47] also found that
242 lubricating oil was a major component of ship exhaust particle emissions.

243

244 Fuel-related metallic contents and engine wear emissions such as Fe, Na, Al and Pb are mainly dominant at
245 MOUDI stages 3 and 4. It is most likely to be that particles larger in diameter (> 100 nm) are strongly associated
246 with fuel-related metallic contents and engine wear emissions. Other metallic elements such as As and Ti show
247 a significant distribution to the MOUDI stage 1 which represents the smallest particles ($D_p < 10$ nm). Therefore,
248 it can be concluded that the smallest particles ($D_p < 10$ nm) are most likely to be linked with elements from the
249 combustion of dust in the air such as Ti and As. However further work is required to confirm this hypothesis
250 because any particles < 10 nm would have a different origin to the larger ones as their composition and formation
251 mechanisms are significantly different.

252



253

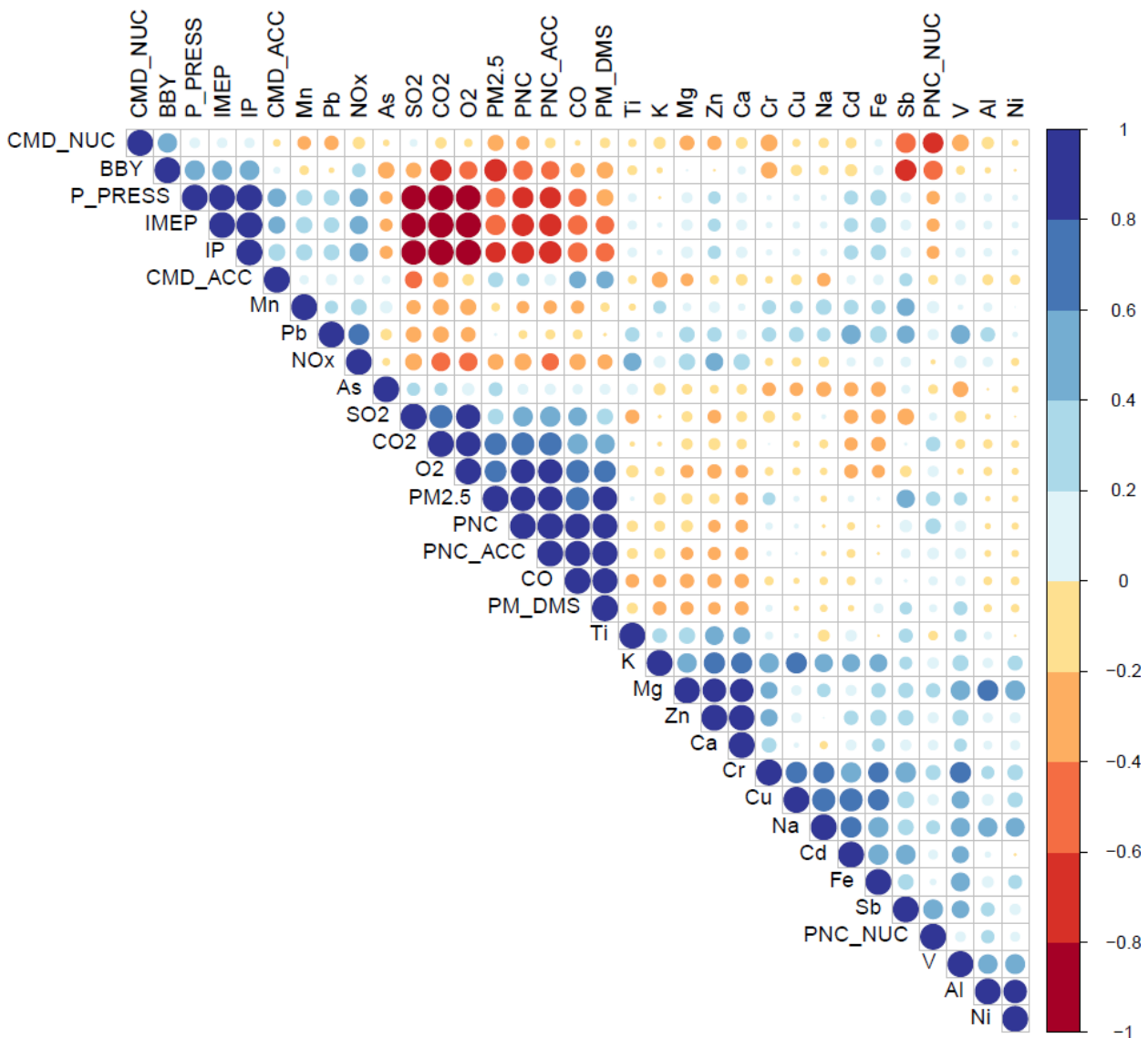
254 **Fig. 3.** Metallic element concentration distributions at different MOUDI stages. The results at each MOUDI
 255 stage were averaged for the all of engine load conditions and tested fuels in the total of ninety-two samples.

256

257 3.3. The correlation between the measured engine performance and emission variables

258 Fig. 4 shows the correlation between the measured engine performance and emission variables where Table S10
 259 provides a full listing of the abbreviations used for variables, along with their units. However, it should be noted
 260 that metallic element concentrations are in mg/m^3 . All of engine load conditions (25 and 50%) and tested fuels
 261 in the total of twenty-three samples were used to plot this figure. Fig. 4 shows that the group of variables
 262 including indicated power (IP), indicated mean effective pressure (IMEP), maximum in-cylinder pressure
 263 (P_PRESS), NO_x and engine blow-by (BBY) are strongly correlated. It is clear that higher engine loads resulted
 264 in an increase in engine combustion chamber temperature and pressure, consequently leading to higher NO_x
 265 emissions and a larger flow of exhaust gas leaking (blow by) through the engine piston rings into the engine
 266 crankcase. Anti-correlated variables with these in the above-mentioned group consist of O_2 , CO_2 , particle
 267 number concentration in the accumulation mode (PNC_ACC), total particle number concentration (PNC), SO_2 ,
 268 CO, $\text{PM}_{2.5}$ and particle mass measured by the DMS500 (PM_DMS). These variables are believed that having a
 269 strong association with low engine load condition which typically represents sub-optimum working conditions.
 270 These conditions can lead to incomplete combustion, consisting of both partially burnt fuel and lubricating oil,
 271 leading to increased concentrations of CO and particle mass and number concentration. This result is in agree-
 272 ment with previous on-board ship emission measurements [14]. Interestingly, O_2 shows an inverse correlation
 273 NO_x and a correlation with CO_2 as can be seen in Fig. 4. It is expected that a direct correlation between O_2 and

274 NO_x as investigated in a previous study [2] and an inverse correlation between O₂ and CO₂ as found in our previous
 275 work [14]. However, the presence of high levels of S in the fuel is well known to significantly alter all emissions
 276 because of the presence of SO_x, which acts as a sink for O₂ and supports increased particle formation.
 277

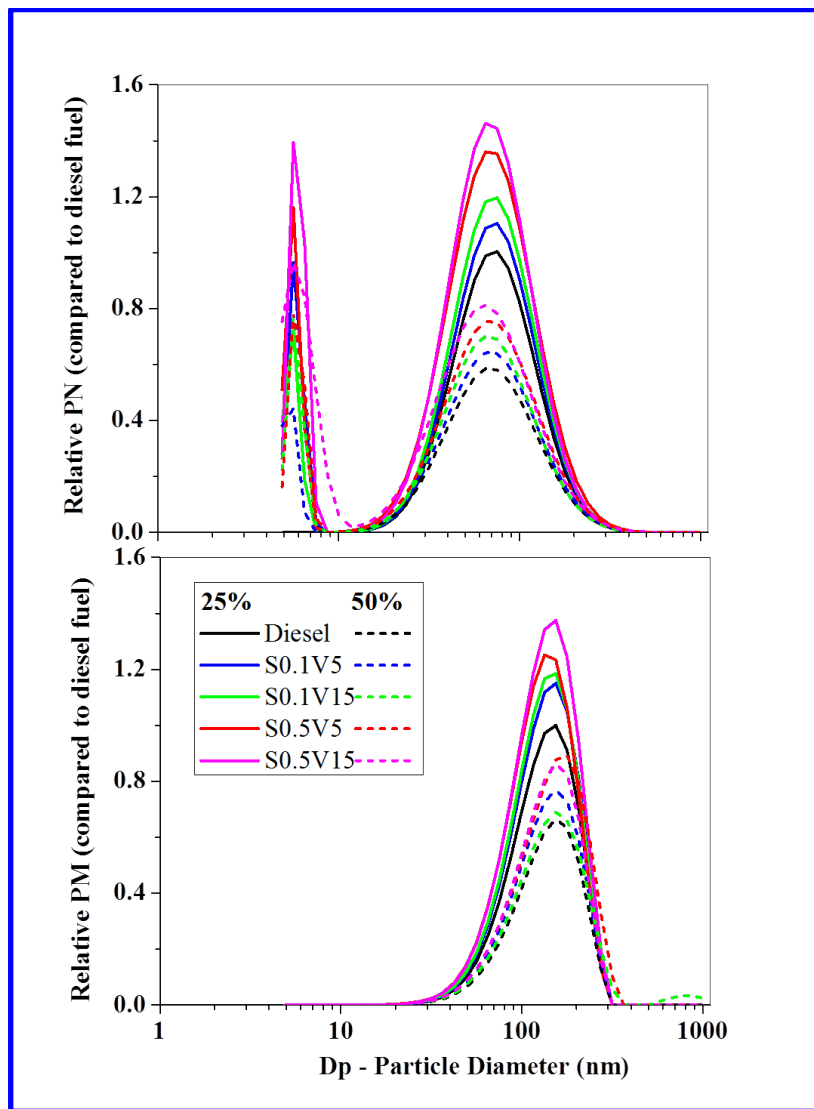


278 **Fig. 4.** Correlation matrix of measured engine performance and emission variables. All of engine load
 279 conditions (25 and 50%) and tested fuels in the total of twenty-three samples were used to plot this figure.
 280

281
 282 Fig. 4 also indicates a strong link between high fuel S content and particulate matter. Higher fuel S content
 283 generally resulted in higher SO₂ emissions which show a correlation with particle mass and number emissions.
 284 In addition, fuel S content S and BBY are anti-correlated on Fig. 4. High S content in the fuel is associated with
 285 higher viscosity and lubricity, as shown in Table 1. Such higher viscosity is linked to lower engine blow-by
 286 because a better seal against combustion gas leakage will be achieved on the piston rings and the piston-cylinder
 287 interaction generally [48]. A positive correlation of engine blow-by and IP, IMEP and P-PRESS is clearly
 288 observed in Fig. 3, which is completely consistent with normal engine operation.
 289

290 **3.4. Particle sized distributions**

291 Fig. 5 shows the particle number and mass size distributions for tested fuels at two different engine load
 292 conditions (25 and 50%). Relative concentration results for both PN and PM to the reference diesel at 25% load
 293 were used in the present study in order to investigate the effects of fuel compositions (S and V contents) and
 294 engine load conditions. It can be seen in Fig. 5 that bimodal for particle number size distributions were observed
 295 for the tested fuels containing S content. No particles in nucleation mode were found in the reference diesel.
 296 Higher PN and PM concentrations observed for the spiked fuels than diesel, are most likely due to the fuel S
 297 and V content. These fuel components will be burned to form sulphur and vanadium oxides which are attributed
 298 to an increase both PN and PM. This is in agreement with correlation results presented in Fig. 4, which show a
 299 correlation between fuel (S and V) content and particulate matter emissions (PN and PM). Fig. 4 also shows a
 300 strong effect of engine load conditions on particle emissions. Higher engine load condition results in lower
 301 particle number and mass emissions. Effects of engine load conditions on exhaust particle emissions also
 302 discussed thoroughly in the present study (Section 3.3). The PN concentration in $\#/cm^3$ and PM in mg/m^3 at two
 303 different engine load conditions (25 and 50%) can be seen in a previous study [18].



304
 305 **Fig. 5.** Relative particle number and mass size distributions for reference diesel and spiked fuels at different
 306 engine load conditions (25 and 50%).

307 **4. Conclusions**

308 This study clearly showed that the most sources of metallic elements in diesel particulate matter emissions
309 originate from fuel, lubricating oil, engine wear and ambient dust in the air. Metallic solid ultrafine-particles
310 ($D_p < 100$ nm) are strongly associated with metallic compounds derived from lubricating oil (Ca, Zn, Mg and
311 K), while the fuel related metallic compounds and engine wear emissions are represented in the accumulation
312 mode particle fraction (> 100 nm). Air Dust related metallic element concentrations (As, Ti) are low but they
313 are linked to the significant contribution to the smallest particles ($D_p < 10$ nm). Correlation matrices were
314 calculated in order to investigate the correlation between variables such as metallic elements, the measured
315 engine performance and engine emission parameters. It was found that there was a strong effect of engine load
316 conditions on particle number and mass emissions. Moreover, results from the present study also indicate a
317 strong link between high fuel S content and particulate matter.

318 **Acknowledgements**

319 The first author gratefully acknowledges the financial support from the Government of Vietnam for a PhD
320 scholarship. The authors would also like to acknowledge: the software developer, Mr. Andrew Elder from
321 DynoLog Dynamometer Pty Ltd; laboratory assistance from Mr. Noel Hartnett; QUT staff and colleagues for
322 their support and guidance. In addition, we gratefully acknowledge the anonymous reviewer who suggested the
323 use of the correlation matrix for this analysis.

324

325 **Appendix A. Supplementary data**

326 Supplementary data associated with this article can be found, in the online version, at
327 <https://www.journals.elsevier.com/fuel>

328 **References**

- 329 [1] Eyring V. Emissions from international shipping: 2. Impact of future technologies on scenarios until
330 2050. *J Geophys Res* 2005;110(D17).
- 331 [2] Mueller L, Jakobi G, Czech H, Stengel B, Orasche J, Arteaga-Salas JM, et al. Characteristics and
332 temporal evolution of particulate emissions from a ship diesel engine. *Appl Energy* 2015;155:204-17.
- 333 [3] Eyring V, Isaksen ISA, Berntsen T, Collins WJ, Corbett JJ, Endresen O, et al. Transport impacts on
334 atmosphere and climate: shipping. *Atmos Environ* 2010;44(37):4735-71.
- 335 [4] Winnes H, Moldanová J, Anderson M, Fridell E. On-board measurements of particle emissions from
336 marine engines using fuels with different sulphur content. *Proc Inst Mech Eng Part M J Eng Marit
337 Environ* 2016;230(1):45-54.
- 338 [5] Anderson M, Salo K, Hallquist ÅM, Fridell E. Characterization of particles from a marine engine
339 operating at low loads. *Atmos Environ* 2015;101(0):65-71.
- 340 [6] Moldanová J, Fridell E, Popovicheva O, Demirdjian B, Tishkova V, Faccineto A, et al. Characterisation
341 of particulate matter and gaseous emissions from a large ship diesel engine. *Atmos Environ*
342 2009;43(16):2632-41.
- 343 [7] Di Natale F, Carotenuto C. Particulate matter in marine diesel engines exhausts: emissions and control
344 strategies. *Trans Res Part D Trans Environ* 2015;40:166-91.
- 345 [8] Ristovski ZD, Miljevic B, Surawski NC, Morawska L, Fong KM, Goh F, et al. Respiratory health effects
346 of diesel particulate matter. *Respirology* 2012;17(2):201-12.
- 347 [9] IARC. Diesel Engine Exhaust Carcinogenic; 2012; [https://www.iarc.fr/en/media-](https://www.iarc.fr/en/media-centre/pr/2012/pdfs/pr213_E.pdf)
348 [centre/pr/2012/pdfs/pr213_E.pdf](https://www.iarc.fr/en/media-centre/pr/2012/pdfs/pr213_E.pdf).
- 349 [10] Corbett JJ, Winebrake JJ, Green EH, Kasibhatla P, Eyring V, Lauer A. Mortality from ship emissions: a
350 global assessment. *Environ Sci Technol* 2007;41(24):8512–8.
- 351 [11] Andersson C, Bergström R, Johansson C. Population exposure and mortality due to regional
352 background PM in Europe – Long-term simulations of source region and shipping contributions. *Atmos
353 Environ* 2009;43(22–23):3614-20.
- 354 [12] Corbett JJ. Updated emissions from ocean shipping. *J Geophys Res* 2003;108(D20).
- 355 [13] Blasco J, Duran-Grados V, Hampel M, Moreno-Gutierrez J. Towards an integrated environmental risk
356 assessment of emissions from ships' propulsion systems. *Environ Int* 2014;66:44-7.
- 357 [14] Chu-Van T, Ristovski ZD, Pourkhesalian AM, Rainey T, Garaniya V, Abbassi R, et al. On-board
358 measurements of particle and gaseous emissions from a large cargo vessel in different operating
359 conditions. *Environ Pollut* 2017;237:832-41.
- 360 [15] Chu Van T, Ramirez J, Rainey T, Ristovski Z, Brown RJ. Global impacts of recent IMO regulations on
361 marine fuel oil refining processes and ship emissions. *Trans Res Part D Trans Environ* 2019;70:123-34.
- 362 [16] Agrawal H, Malloy QGJ, Welch WA, Wayne Miller J, Cocker Iii DR. In-use gaseous and particulate
363 matter emissions from a modern ocean going container vessel. *Atmos Environ* 2008;42(21):5504-10.
- 364 [17] Celo V, Dabek-Zlotorzynska E, McCurdy M. Chemical characterization of exhaust emissions from
365 selected Canadian marine vessels: the case of trace metals and lanthanoids. *Environ Sci Technol*

- 366 2015;49(8):5220-6.
- 367 [18] Chu Van T, Ristovski Z, Surawski N, Bodisco TA, Rahman SMA, Alroe J, et al. Effect of sulphur and
368 vanadium spiked fuels on particle characteristics and engine performance of auxiliary diesel engines.
369 Environ Pollut 2018;243:1943-51.
- 370 [19] Lindstad HE, Rehn CF, Eskeland GS. Sulphur abatement globally in maritime shipping. Trans Res Part
371 D Trans Environ 2017;57:303-13.
- 372 [20] Brynolf S, Magnusson M, Fridell E, Andersson K. Compliance possibilities for the future ECA
373 regulations through the use of abatement technologies or change of fuels. Trans Res Part D Trans
374 Environ 2014;28:6-18.
- 375 [21] Moldanová J, Fridell E, Winnes H, Holmin-Fridell S, Boman J, Jedynska A, et al. Physical and chemical
376 characterisation of PM emissions from two ships operating in European emission control areas. Atmos
377 Meas Tech 2013;6(12):3577-96.
- 378 [22] Viana M, Hammings P, Colette A, Querol X, Degraeuwe B, Vlioger Id, et al. Impact of maritime
379 transport emissions on coastal air quality in Europe. Atmos Environ 2014;90(0):96-105.
- 380 [23] Sippula O, Stengel B, Sklorz M, Streibel T, Rabe R, Orasche J, et al. Particle emissions from a marine
381 engine: chemical composition and aromatic emission profiles under various operating conditions.
382 Environ Sci Technol 2014;48(19):11721-9.
- 383 [24] Petzold A, Weingartner E, Hasselbach J, Lauer P, Kurok C, Fleischer F. Physical properties, chemical
384 composition, and cloud forming potential of particulate emissions from a marine diesel engine at various
385 load conditions. Environ Sci Technol 2010;44(10):3800-5.
- 386 [25] Abdul Jameel AG, Elbaz AM, Emwas A-H, Roberts WL, Sarathy SM. Calculation of average molecular
387 parameters, functional groups, and a surrogate molecule for heavy fuel oils using 1H and 13C nuclear
388 magnetic resonance spectroscopy. Energy Fuels 2016;30(5):3894-905.
- 389 [26] Hsieh PY, Abel KR, Bruno TJ. Analysis of marine diesel fuel with the advanced distillation curve
390 method. Energy Fuels 2013;27(2):804-10.
- 391 [27] Saiyasitpanich P, Lu M, Keener TC, Liang F, Khang SJ. The effect of diesel fuel sulfur content on
392 particulate matter emissions for a nonroad diesel generator. J Air Waste Manage Assoc 2005;55(7):993-
393 8.
- 394 [28] Ruger CP, Sklorz M, Schwemer T, Zimmermann R. Characterisation of ship diesel primary particulate
395 matter at the molecular level by means of ultra-high-resolution mass spectrometry coupled to laser
396 desorption ionisation—comparison of feed fuel, filter extracts and direct particle measurements. Anal
397 Bioanal Chem 2015;407(20):5923-37.
- 398 [29] Dunning HN, Moore JW, Bieber H, Williams RB. Porphyrin, Nickel, vanadium, and nitrogen in
399 petroleum. J Chem Eng Data 1960;5(4):546-9.
- 400 [30] Zhang Z-H, Balasubramanian R. Effects of cerium oxide and ferrocene nanoparticles addition as fuel-
401 borne catalysts on diesel engine particulate emissions: environmental and health implications. Environ
402 Sci Technol 2017;51(8):4248-58.
- 403 [31] Rahman SMA, Chu-Van T, Hossain FM, Jafari M, Dowell A, Islam MA, et al. Fuel properties and

- 404 emission characteristics of essential oil blends in a compression ignition engine. *Fuel* 2019;238:440-53.
- 405 [32] Marple VA, Rubow KL, Behm SM. A microorifice uniform deposit impactor (MOUDI): description,
406 calibration, and use. *Aerosol Sci Technol* 1991;14(4):434-46.
- 407 [33] Ham WA, Kleeman MJ. Size-resolved source apportionment of carbonaceous particulate matter in
408 urban and rural sites in central California. *Atmos Environ* 2011;45(24):3988-95.
- 409 [34] Biswas S, Verma V, Schauer JJ, Sioutas C. Chemical speciation of PM emissions from heavy-duty diesel
410 vehicles equipped with diesel particulate filter (DPF) and selective catalytic reduction (SCR) retrofits.
411 *Atmos Environ* 2009;43(11):1917-25.
- 412 [35] Yang H-Y, Tseng Y-L, Chuang H-L, Li T-C, Yuan C-S. Chemical fingerprint and source identification
413 of atmospheric fine particles sampled at three environments at the tip of Southern Taiwan. *Aerosol Air
414 Qual Res* 2017;17(2):529-42.
- 415 [36] The R Foundation for Statistical Computing. R version 3.4.0. 2017.
- 416 [37] Wei T, Simko V, Levy M, Xie Y, Jin Y, Zemla J. Visualization of a correlation matrix: corrplot. *The
417 Comprehensive R Archive Network* 2017.
- 418 [38] Crilley LR, Ayoko GA, Stelcer E, Cohen DD, Mazaheri M, Morawska L. Elemental composition of
419 ambient fine particles in urban schools: sources of children's exposure. *Aerosol Air Qual Res*
420 2014;14(7):1906-16.
- 421 [39] Friend AJ, Ayoko GA, Stelcer E, Cohen D. Source apportionment of PM_{2.5} at two receptor sites in
422 Brisbane, Australia. *Environ Chem* 2011;8(6):569-80.
- 423 [40] Celik I, Koc O. An experimental and comparative examination of the effect of biodiesel fuel on engine
424 wear. *Energy Source Part A* 2011;33(15):1451-62.
- 425 [41] Zali MA, Ahmad WKW, Retnam A, Catrina N. Concentration of heavy metals in virgin, used, recovered
426 and waste oil: a spectroscopic study. *Procedia Environ Sci* 2015;30:201-4.
- 427 [42] Rahim MF, Pal D, Ariya PA. Physicochemical studies of aerosols at Montreal Trudeau Airport: the
428 importance of airborne nanoparticles containing metal contaminants. *Environ Pollut* 2019;246:734-44.
- 429 [43] Pirjola L, Karjalainen P, Heikkilä J, Saari S, Tzamkiozis T, Ntziachristos L, et al. Effects of fresh
430 lubricant oils on particle emissions emitted by a modern gasoline direct injection passenger car. *Environ
431 Sci Technol* 2015;49(6):3644-52.
- 432 [44] Gidney JT, Twigg MV, Kittelson DB. Effect of organometallic fuel additives on nanoparticle emissions
433 from a gasoline passenger car. *Environ Sci Technol* 2010;44(7):2562-9.
- 434 [45] Carbone S, Timonen HJ, Rostedt A, Happonen M, Rönkkö T, Keskinen J, et al. Distinguishing fuel and
435 lubricating oil combustion products in diesel engine exhaust particles. *Aerosol Sci Technol* 2019:1-14.
- 436 [46] Martin NR, Kelley P, Klaski R, Bosco A, Moore B, Traviss N. Characterization and comparison of
437 oxidative potential of real-world biodiesel and petroleum diesel particulate matter emitted from a
438 nonroad heavy duty diesel engine. *Sci Total Environ* 2019;655:908-14.
- 439 [47] Eichler P, Müller M, Rohmann C, Stengel B, Orasche J, Zimmermann R, et al. Lubricating oil as a
440 major constituent of ship exhaust particles. *Environ Sci Technol Lett* 2017;4(2):54-8.
- 441 [48] Mitchell BJ, Zare A, Bodisco TA, Nabi MN, Hossain FM, Ristovski ZD, et al. Engine blow-by with

442 oxygenated fuels: a comparative study into cold and hot start operation. Energy 2017;140(Part 1):612-
443 24.
444